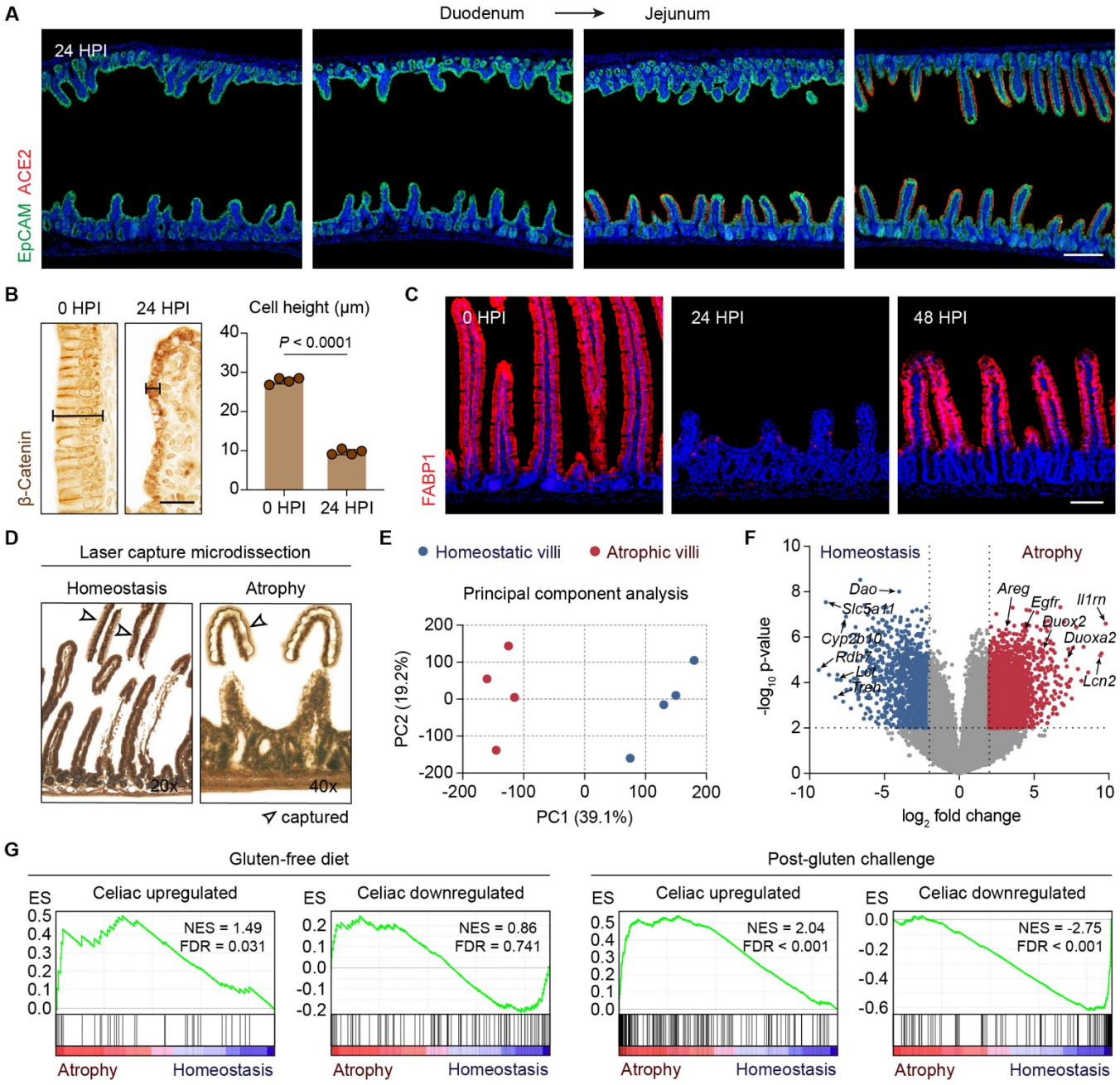

Figure S1. Characterization of villus atrophy-induced epithelial changes, related to Figure 1

(A) Immunofluorescence (IF) for EpCAM (green) and ACE2 (red) in the small intestine from the duodenum to the proximal jejunum at 24 HPI. Bar: 200μm. **(B)** Immunohistochemistry (IHC) for β-Catenin (brown) in a representative villus at the indicated time points (left). Bar: 20μm. Average epithelial cell height across 50 villi based on H&E images was plotted as mean ± SD (right). n=4 mice/group. Significance was determined by unpaired *t*-test. **(C)** IF for FABP1 (red)

at the indicated time points. Bar: 100μm. **(D)** Example of a laser-capture microdissection (LCM) experiment showing isolation of villus epithelial cells (VECs) from the homeostatic and atrophic intestine. Arrowheads indicate captured cells. **(E)** Principal component analysis of bulk transcriptomes from homeostatic VECs and atrophy-induced VECs (aVECs). **(F)** Volcano plot showing differentially expressed genes between homeostatic VECs and aVECs. Significant genes ($p < 0.01$ and fold-change > 2) were color-coded red or blue. **(G)** Gene set enrichment analysis (GSEA) of genes upregulated or downregulated in celiac disease patients on a gluten-free diet (left panel) or post-gluten challenge (right panel) in aVECs compared with homeostatic VECs. Normalized enrichment scores (NES) and false discovery rates (FDR) are shown.

IF and IHC images are representative of at least 3 animals.

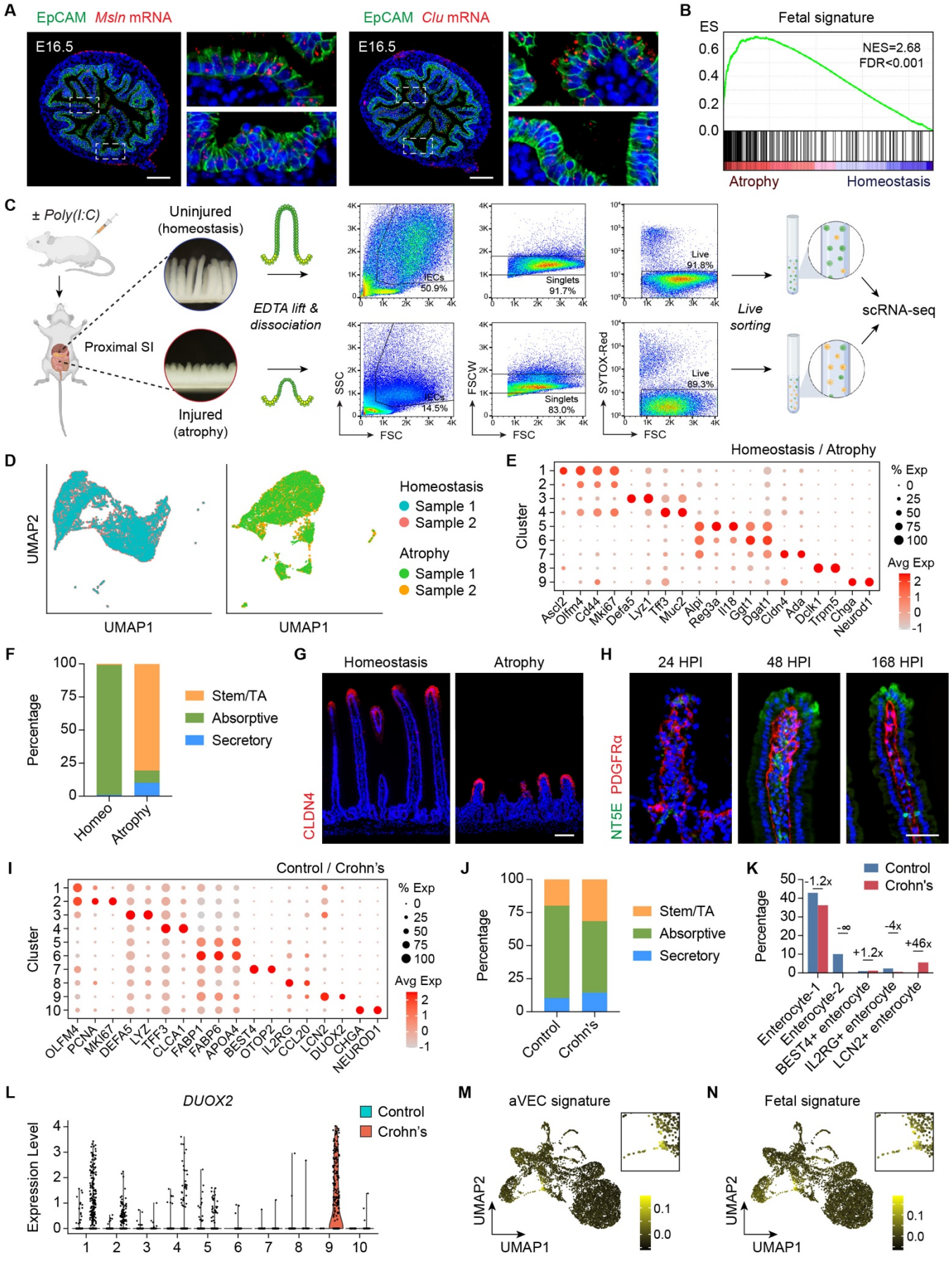
A
EpCAM Msln mRNA
E16.5
EpCAM Clu mRNA
E16.5
B
Fetal signature
ES
NES=2.68
FDR<0.001
Atrophy
Homeostasis
C
± Poly(I:C)
Uninjured
(homeostasis)
Proximal SI
Injured
(atrophy)
EDTA lift &
dissociation
IECs
50.9%
Singlets
91.7%
Live
91.8%
IECs
14.5%
Singlets
83.0%
Live
89.3%
SSC
FSCW
SYTOX-Red
FSC
Live
sorting
scRNA-seq
D
UMAP2
UMAP1
UMAP1
Homeostasis
Sample 1
Sample 2
Atrophy
Sample 1
Sample 2
E
Homeostasis / Atrophy
Cluster
% Exp
Avg Exp
Ascl2
Olfm4
Cd44
Mki67
Defa5
Lyz1
Tff3
Muc2
Alpi
Reg3a
Il18
Ggt1
Dgat1
Cldn4
Ada
Dclk1
Trpm5
Chga
Neurod1
F
Percentage
Stem/TA
Absorptive
Secretory
Homeo
Atrophy
G
Homeostasis
Atrophy
CLDN4
H
24 HPI
48 HPI
168 HPI
NT5E PDGFRα
I
Control / Crohn's
Cluster
% Exp
Avg Exp
OLFM4
PCNA
MKI67
DEFA5
LYZ
TFF3
CLCA1
FABP1
FABP6
APOA4
BEST4
OTOP2
IL2RG
CCL20
LCN2
DUOX2
CHGA
NEUROD1
J
Percentage
Stem/TA
Absorptive
Secretory
Control
Crohn's
K
Control
Crohn's
Percentage
-1.2x
-∞
+1.2x
-4x
+46x
Enterocyte-1
Enterocyte-2
BEST4+ enterocyte
IL2RG+ enterocyte
LCN2+ enterocyte
L
DUOX2
Control
Crohn's
Expression Level
M
aVEC signature
UMAP2
UMAP1
N
Fetal signature
UMAP2
UMAP1

Figure S2. Single-cell analysis of the intestinal epithelium in enteropathy, related to Figure 2

(A) IF/RNAscope *in situ* hybridization for EpCAM (green) and *Msln* or *Clu* (red) in E16.5 intestines. Each red dot represents a single mRNA molecule. **(B)** GSEA of a fetal signature in aVECs compared with homeostatic VECs. **(C)** Schematic of single-cell RNA sequencing (scRNA-seq) protocol. Intestinal epithelial cells (IECs) from the homeostatic and atrophic intestine were isolated by EDTA treatment, enzymatically dissociated, and sorted based on the gating strategy shown. **(D)** UMAP visualization of scRNA-seq libraries from two independent homeostasis samples and two independent villus atrophy samples reveals minimal batch-to-batch variation. **(E)** Dot plot of cell type-specific and enterocyte zonation markers in the homeostasis vs atrophy IEC scRNA-seq dataset. **(F)** Proportion of stem/progenitor cells, absorptive enterocytes, and secretory cells (i.e., Paneth, goblet, enteroendocrine, and tuft cells) in the homeostatic and atrophic intestine based on scRNA-seq clusters. **(G)** IF for CLDN4 (red), a villus tip marker, in the homeostatic and atrophic intestine. **(H)** IF for NT5E (green) and PDGFRα (red) in a representative villus at the indicated time points. **(I)** Dot plot of cell type-specific and cluster-defining markers in the healthy control vs pediatric Crohn's disease IEC scRNA-seq dataset. **(J and K)** Proportion of stem/progenitor cells, absorptive enterocytes, and secretory cells (i.e., Paneth, goblet, and enteroendocrine cells) in healthy controls and pediatric Crohn's disease patients based on scRNA-seq clusters (J). Proportion of enterocyte subsets and the relative fold difference between healthy controls and pediatric Crohn's disease patients (K). *LCN2*$^{+}$ enterocytes (cluster 9) uniquely arise in Crohn's disease. **(L)** Expression of *DUOX2* in each cluster separated by disease status. Each black dot represents one cell. *DUOX2* is predominantly expressed in Crohn's-associated *LCN2*$^{+}$ enterocytes (cluster 9). **(M and N)** Expression of the aVEC (M) and mouse fetal (N) signature was overlaid on the UMAP plot. Highest expressors (yellow-colored cells) were concentrated in *DUOX2*$^{+}$ cells.

Bars: (A and G) 100μm; (H) 50μm. IF and RNAscope images are representative of at least 3 animals.

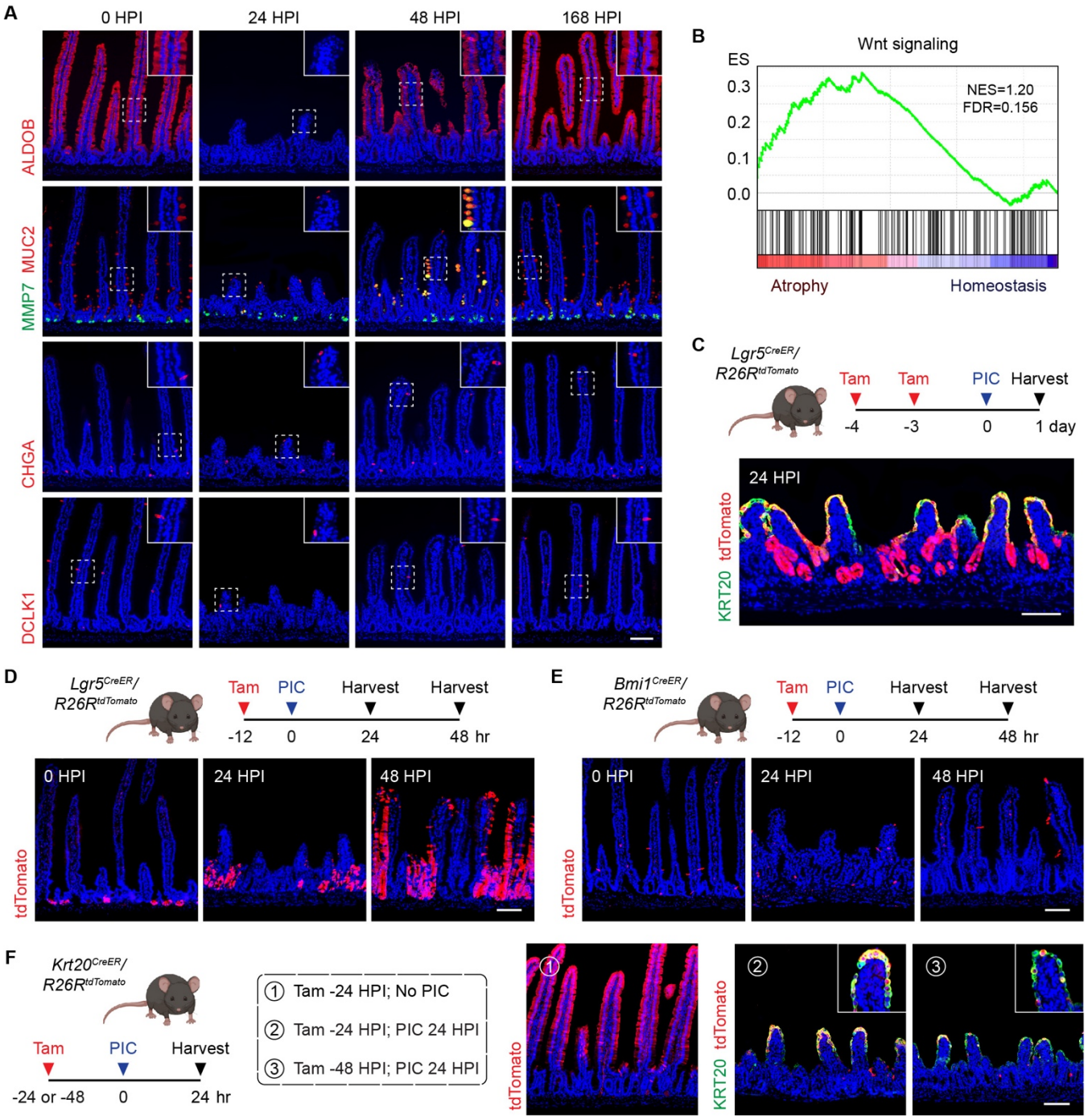

Figure S3. Lineage and turnover dynamics during villus injury-repair, related to Figure 3

(A) IF for cell lineage markers at the indicated time points. Expression of ALDOB (enterocyte), MUC2 (goblet cell), MMP7 (Paneth cell), CHGA (enteroendocrine cell), and DCLK1 (tuft cell) was examined. ALDOB expression is lost during villus atrophy and $MUC2^{+}MMP7^{+}$ intermediate cells arise during villus regeneration. Images are representative of at least 3 animals. Bar: 100μm. **(B)** GSEA of the Wnt signaling pathway (KEGG mmu04310) in aVECs compared with

homeostatic VECs. **(C-F)** Lineage tracing of pre-injury LGR5-progeny cells, LGR5^{+} intestinal stem cells (ISCs), BMI1^{+} cells, and KRT20^{+} cells. LGR5-progeny cells were labeled following tamoxifen-mediated tracing of ISCs 3-4 days prior to poly(I:C) injection in *Lgr5*^{CreER}*/R26R*^{tdTomato} mice (C). LGR5^{+} ISCs and BMI1^{+} cells were labeled with tamoxifen 12 h prior to poly(I:C) injection in *Lgr5*^{CreER}*/R26R*^{tdTomato} and *Bmi1*^{CreER}*/R26R*^{tdTomato} mice, respectively (D and E). KRT20^{+} cells were labeled with tamoxifen either 24 h or 48 h prior to poly(I:C) injection in *Krt20*^{CreER}*/R26R*^{tdTomato} mice (F). The contribution of each cell population to aVECs at 24 HPI and villus regeneration at 48 HPI are shown. LGR5-progenies are the major source of aVECs (by colocalization with KRT20) with possible or minor contribution of pre-injury BMI1^{+} cells and KRT20^{+} cells.

All bars: 100μm. IF images are representative of at least 4 animals.

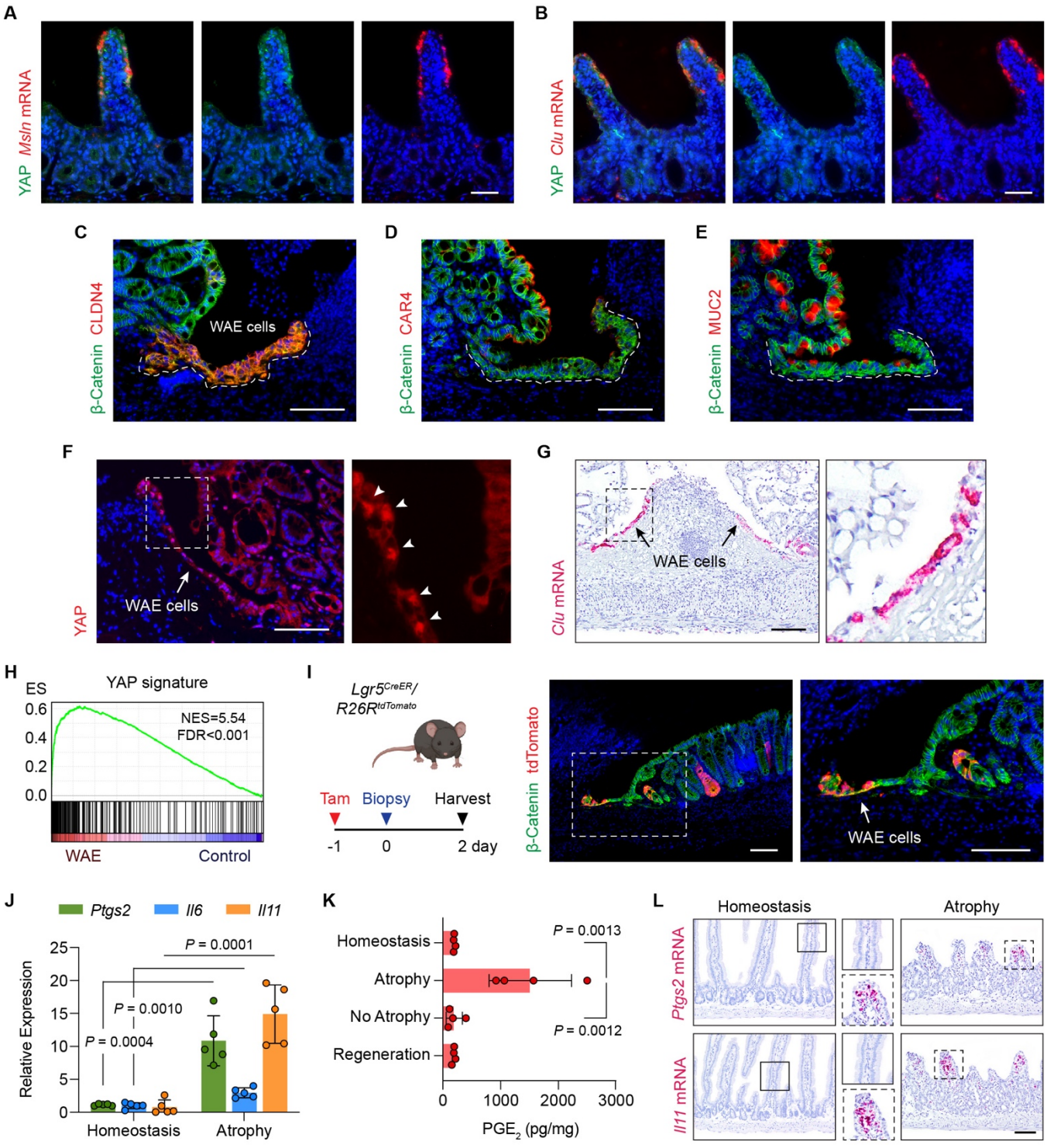

Figure S4. Activation of YAP during adaptive differentiation, related to Figure 4

(A and B) IF/RNAscope for YAP (green) and *Msln* (A) or *Clu* (B) (red) in the atrophic intestine. **(C-E)** IF for CLDN4 (C), CAR4 (D), and MUC2 (E) in day 2 colonic biopsy wounds. β-Catenin (green) marks epithelial cells. Serial sections were stained to examine the expression of CAR4

(colonocyte marker) and MUC2 (goblet cell marker) in CLDN4^{+} wound-associated epithelial (WAE) cells (white dashed line). **(F and G)** IF for YAP (F) and RNAscope for *Clu* (G) in day 2 colonic biopsy wounds reveal nuclear YAP expression and high *Clu* expression in WAE cells (arrows). **(H)** GSEA of YAP target genes in WAE cells (day 2 and 4 post-injury) compared with control cells (adjacent uninjured surface epithelium and crypts on day 2 and 4 post-injury). **(I)** Fate mapping of LGR5^{+} lineage cells following colonic biopsy injury. LGR5^{+} ISCs were labeled with tamoxifen 1 day prior to injury in *Lgr5*^{CreER}*/R26R*^{tdTomato} mice. LGR5^{+} lineage cells contribute to the generation of WAE cells (white arrow) on day 2 post-injury. **(J)** qPCR analysis of *Ptgs2* and gp130 cytokines (*Il6*, *Il11*) in whole tissue lysates from the homeostatic and atrophic intestine. Values were normalized to the lowest expressing sample. n=5 mice/group. **(K)** PGE_2 levels were measured by ELISA in whole tissue lysates from the homeostatic, atrophic (24 HPI), non-atrophic (distal uninjured region at 24 HPI), and regenerating (48 HPI) intestine. n=4 mice/group. **(L)** RNAscope for *Ptgs2* (top) and *Il11* (bottom) in the homeostatic and atrophic intestine. *Ptgs2* and *Il11* transcripts are induced in the stroma of atrophic villi.

All values in (J) and (K) are displayed as mean ± SD. Unpaired *t*-test in (J). One-way ANOVA and Tukey's multiple comparisons test in (K). Bars: (A and B) 50μm; (C-G, I, and L) 100μm. IF and RNAscope images are representative of at least 3 animals.

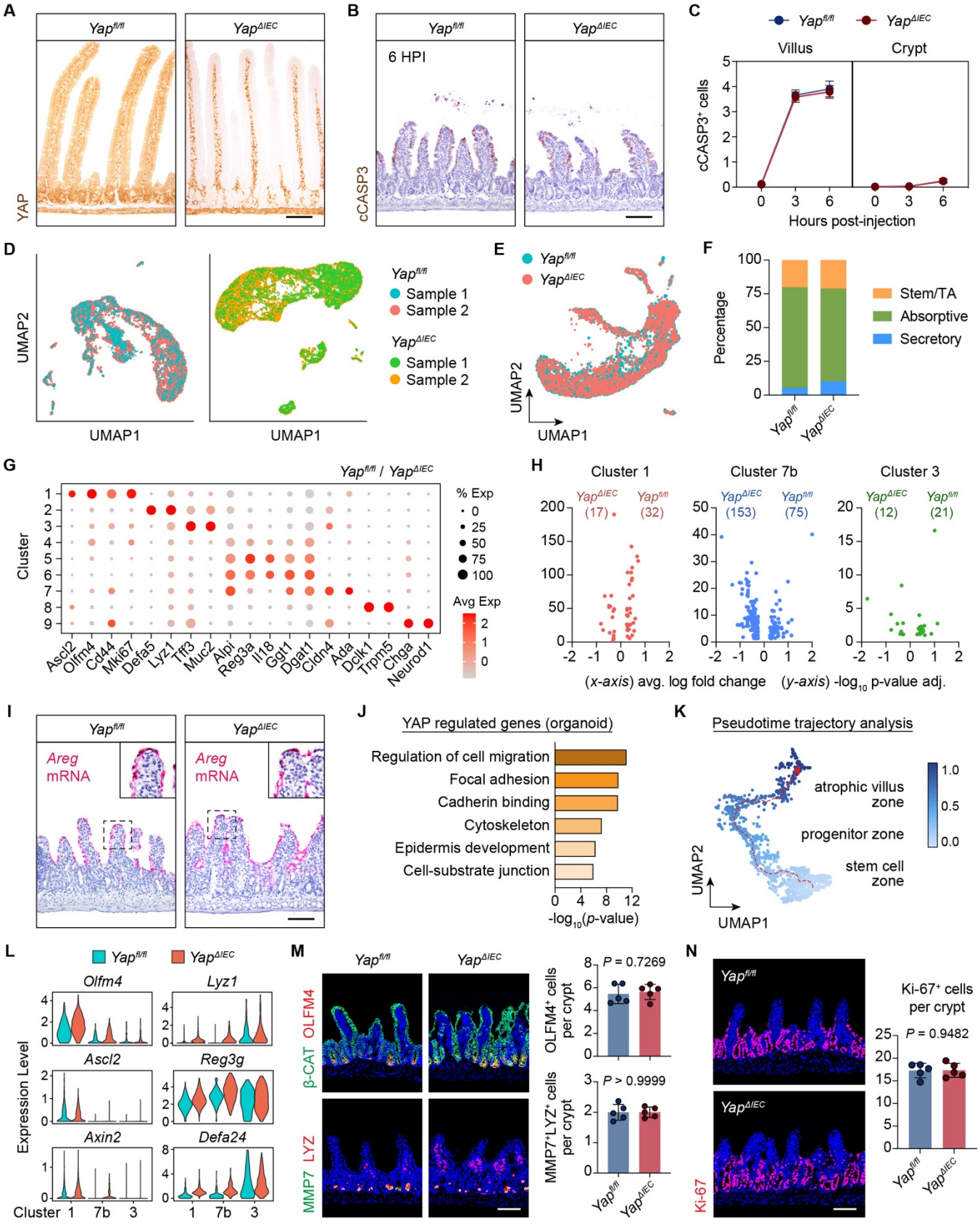
A
Yap^fl/fl
Yap^ΔIEC
YAP
B
6 HPI
cCASP3
C
Villus
Crypt
cCASP3+ cells
Hours post-injection
D
UMAP2
UMAP1
Sample 1
Sample 2
E
F
Percentage
Stem/TA
Absorptive
Secretory
G
Cluster
% Exp
Avg Exp
Ascl2
Olfm4
Cd44
Mki67
Defa5
Lyz1
Tff3
Muc2
Alpi
Reg3a
Il18
Ggt1
Dgat1
Cldn4
Ada
Dclk1
Trpm5
Chga
Neurod1
H
Cluster 1
Cluster 7b
Cluster 3
(x-axis) avg. log fold change
(y-axis) -log10 p-value adj.
I
Areg mRNA
J
YAP regulated genes (organoid)
Regulation of cell migration
Focal adhesion
Cadherin binding
Cytoskeleton
Epidermis development
Cell-substrate junction
-log10(p-value)
K
Pseudotime trajectory analysis
atrophic villus zone
progenitor zone
stem cell zone
L
Olfm4
Lyz1
Ascl2
Reg3g
Axin2
Defa24
Expression Level
Cluster 1 7b 3
M
β-CAT OLFM4
MMP7 LYZ
OLFM4+ cells per crypt
P = 0.7269
MMP7+LYZ+ cells per crypt
P > 0.9999
N
Ki-67
Ki-67+ cells per crypt
P = 0.9482

Figure S5. Single-cell analysis of the YAP-deficient intestinal epithelium, related to Figure 5

(A) IHC for YAP (brown) in the homeostatic intestine from *Yap*$^{fl/fl}$ and *Yap*$^{\Delta IEC}$ mice validating the loss of YAP expression in the intestinal epithelium in *Yap*$^{\Delta IEC}$ mice. **(B and C)** IHC for cleaved-caspase 3 (cCASP3) (brown) at 6 HPI (B). Average number of cCASP3^{+} cells across 50 villi/crypts at the indicated time points in *Yap*$^{fl/fl}$ and *Yap*$^{\Delta IEC}$ mice was plotted as mean ± SD (C). n=3 mice/group. No significant difference was observed by two-way ANOVA with Tukey's multiple comparisons test. **(D)** UMAP visualization of scRNA-seq libraries from two independent *Yap*$^{fl/fl}$ samples and two independent *Yap*$^{\Delta IEC}$ samples reveals minimal batch-to-batch variation. **(E and F)** UMAP visualization of IECs from *Yap*$^{fl/fl}$ and *Yap*$^{\Delta IEC}$ mice with similar level of damage (containing roughly equivalent amount of the atrophic and distal non-atrophic regions of the gut) colored by genotype (E). Proportion of stem/progenitor cells, absorptive enterocytes, and secretory cells (i.e., Paneth, goblet, enteroendocrine, and tuft cells) based on scRNA-seq clusters (F). **(G)** Dot plot of cell type-specific and enterocyte zonation markers in the *Yap*$^{fl/fl}$ vs *Yap*$^{\Delta IEC}$ IEC scRNA-seq dataset. **(H)** Differentially expressed genes between *Yap*$^{fl/fl}$ and *Yap*$^{\Delta IEC}$ cells were plotted for stem/progenitor cells (cluster 1), atrophy-induced enterocytes (cluster 7b), and goblet cells (cluster 3). *Yap* deficiency had the greatest impact on gene expression in atrophy-induced enterocytes. **(I)** RNAscope for *Areg* in the atrophic intestine from *Yap*$^{fl/fl}$ and *Yap*$^{\Delta IEC}$ mice. **(J)** Pathway analysis of the top 300 YAP regulated genes in intestinal organoids. **(K)** Pseudotime analysis of *Yap*$^{fl/fl}$ and *Yap*$^{\Delta IEC}$ IECs associated with villus atrophy based on single cell transcriptomes. Cells were colored by progression through a pseudotime differentiation trajectory (from the stem cell zone to the atrophic villus zone). Red dashed arrow indicates direction of fate progression. **(L)** Expression of stem cell (*Olfm4*, *Ascl2*), Wnt (*Axin2*), and Paneth cell (*Lyz1*, *Reg3g, Defa24*) markers in the indicated clusters separated by genotype. **(M and N)** IF and quantification of OLFM4^{+} ISCs (M, top), MMP7^{+}LYZ^{+} Paneth cells (M, bottom), and Ki-67^{+} proliferating cells (N) in the crypt. Average number of cells across 30 crypts was plotted as mean ± SD. n=5 mice/group. Significance was determined by unpaired *t*-test.

All bars: 100μm. IHC, RNAscope, and IF images are representative of at least 3 animals.

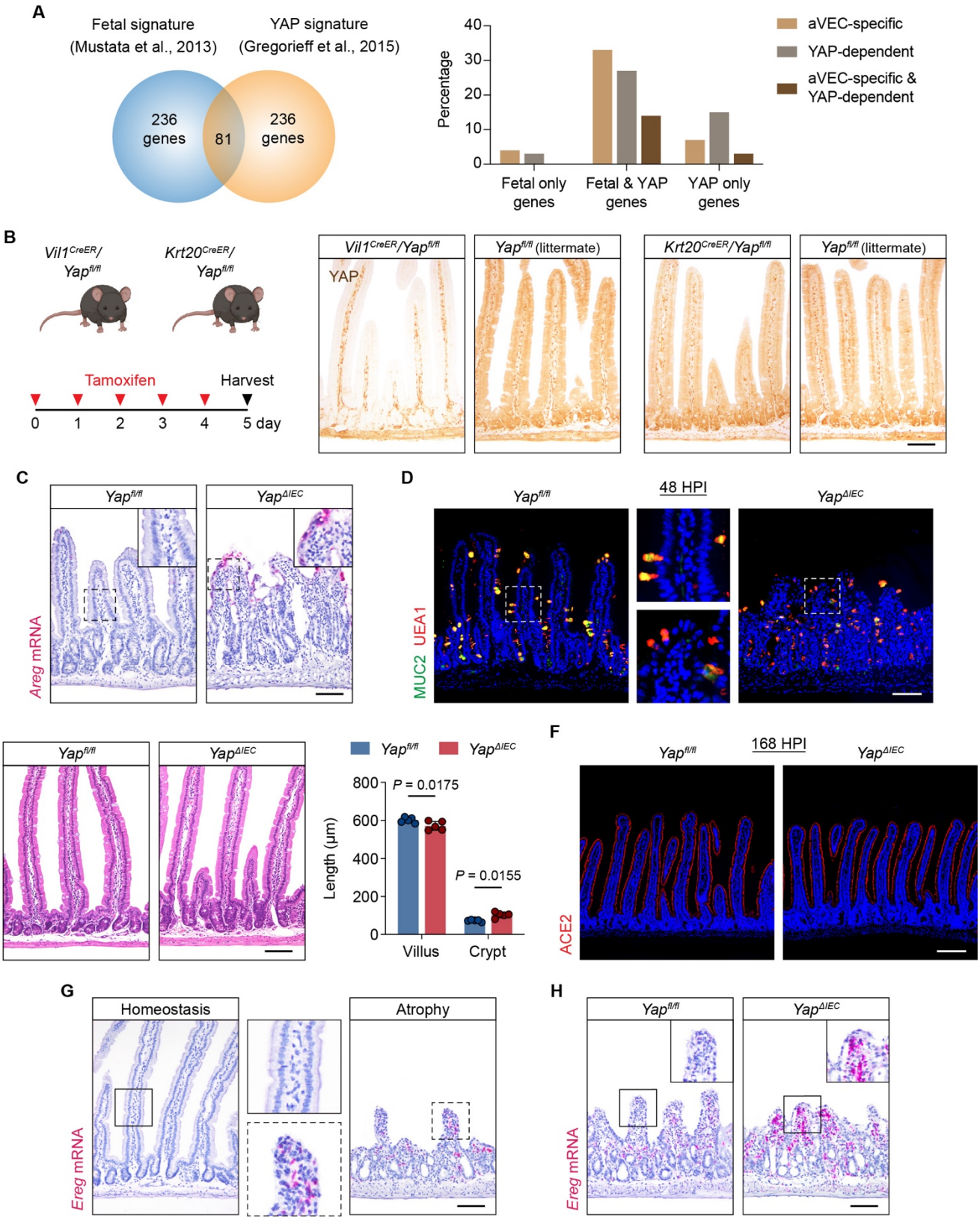

Figure S6. Consequence of YAP deficiency following villus injury, related to Figure 6

(A) Venn diagram of all the fetal signature genes (317 total) and the top 317 YAP signature genes reveals 81 overlapping targets (left). Every gene from this merged dataset (indicated as fetal only, fetal and YAP, or YAP only genes) was assessed for its specificity as an aVEC marker (as determined by our scRNA-seq data in Figure 2) and its dependency on YAP in aVECs (as determined by our scRNA-seq data in Figure 5). Percentage of genes that meet these criteria was plotted (right). **(B)** *Vil1*^{CreER}/*Yap*$^{fl/fl}$, *Krt20*^{CreER}/*Yap*$^{fl/fl}$, and *Yap*$^{fl/fl}$ littermate control mice were given 5 consecutive injections of tamoxifen and examined on the 6th day (left). IHC for YAP (brown) in the homeostatic intestine from these mice (right). Loss of YAP expression was seen in *Vil1*^{CreER}/*Yap*$^{fl/fl}$ mice (positive control) but not in *Krt20*^{CreER}/*Yap*$^{fl/fl}$ mice. **(C)** RNAscope for *Areg* in the regenerating intestine at 48 HPI from *Yap*$^{fl/fl}$ and *Yap*$^{\Delta IEC}$ mice. **(D)** IF for MUC2 (green) and UEA1 (red) in the regenerating intestine at 48 HPI from *Yap*$^{fl/fl}$ and *Yap*$^{\Delta IEC}$ mice. **(E)** H&E images of the regenerating intestine at one-week post-injury from *Yap*$^{fl/fl}$ and *Yap*$^{\Delta IEC}$ mice (left). Average villus/crypt length across 50 villi/crypts was plotted as mean ± SD (right). n=5 mice/group. Significance was determined by two-way ANOVA and Sidak's multiple comparisons test. **(F)** IF for ACE2 in the regenerating intestine at 168 HPI from *Yap*$^{fl/fl}$ and *Yap*$^{\Delta IEC}$ mice. **(G and H)** RNAscope for *Ereg* in the homeostatic and atrophic intestine from wild-type mice (G) and the atrophic intestine from *Yap*$^{fl/fl}$ and *Yap*$^{\Delta IEC}$ mice (H). *Ereg* expression is induced during villus atrophy in the stroma, which is even more pronounced in *Yap*$^{\Delta IEC}$ atrophic villi.

Bars: (B-E, G, and H) 100μm; (F) 200μm. IHC, RNAscope, IF, and H&E images are representative of at least 3 animals. See also Table S2.